

# A Multifunctional Dual-Salt Localized High-Concentration Electrolyte for Fast Dynamic High-Voltage Lithium Battery in Wide Temperature Range

Shuangshuang Lin, Haiming Hua, Pengbin Lai, and Jinbao Zhao\*

In this work, a multifunctional 2m dual-salt sulfolane (TMS)/ethyl acetate (EA)-based localized high-concentration electrolyte (LHCE) with 10 wt% fluoro-carbonate (FEC) is reported. Its incorporation into a  $\text{Li}||\text{Ni}_{0.5}\text{Co}_{0.2}\text{Mn}_{0.3}\text{O}_2$  battery enables it to maintain nearly 89% capacity retention after 200 cycles with 1 C ( $200 \text{ mA g}^{-1}$ ) charge/discharge current density charged to 4.6 V at 25 °C, showing good high-voltage cyclic stability. A superior 10 C high-rate performance with 65% ( $\approx 130 \text{ mAh g}^{-1}$ ) specific capacity is also achieved. Furthermore, it still remains a liquid and exhibits good ionic conductivity even at  $-80 \text{ }^\circ\text{C}$ , and enables  $\text{Li}||\text{Ni}_{0.5}\text{Co}_{0.2}\text{Mn}_{0.3}\text{O}_2$  batteries to deliver more than 50% of their room-temperature capacity at  $-40 \text{ }^\circ\text{C}$  and remains stable for over 200 cycles under the same condition as before, realizing outstanding low-temperature fast-charging/discharging performance. It also demonstrates compatibility with both lithium metal and graphite anode. All in all, this work provides a new idea for the design of a fast-dynamic, high-voltage, and low-temperature lithium battery electrolyte. The findings of this work indicate that LHCEs made directly from the optimal high-concentration electrolyte are not the most suitable approach, combining the diluent with an additive is necessary and effective.

## 1. Introduction

Lithium-ion batteries<sup>[1]</sup> are widely used in small electronic devices such as mobile phones and notebook computers due to their high energy density,<sup>[2]</sup> long cycle life,<sup>[3]</sup> and no memory effect. They are also popularized in large-scale energy storage fields such as smart grids and electric vehicles. As the market share of power batteries continues to increase, people have shown a more urgent need for higher energy density storage devices. To meet the need, we can develop high-voltage cathode materials such as high-voltage  $\text{LiCoO}_2$ <sup>[4]</sup> high-nickel  $\text{LiNi}_x\text{Co}_y\text{Mn}_z\text{O}_2$ <sup>[5]</sup> and lithium-rich cathode materials<sup>[6]</sup> and

high-energy density anode materials such as lithium metal,<sup>[7]</sup> silicon-based anode,<sup>[8]</sup> and so on. Of course, the electrolyte,<sup>[9]</sup> as the link between cathode and anode, also plays a very important role in the battery system. However, traditional commercial carbonate electrolyte<sup>[10]</sup> only has limited oxidation stability (about 4.3 V), which limits its application in the high-voltage battery field. What's more, the electrode materials have slower dynamics under low temperature<sup>[11]</sup> conditions, thus delivering less capacity. Therefore, it is more important to develop an electrolyte that can be compatible with high-voltage materials in wide temperature range. The sulfone solvent<sup>[12]</sup> is expected to be an ideal solvent for high-voltage electrolyte due to its low price and high oxidation stability. Tan et al.<sup>[13]</sup> reported that the electrochemical window of methyl ethyl sulfone (EMS) can reach up to 5.9 V. While the high viscosity of sulfone solvent also limits its further application, and the addition

of cosolvent is a very effective method. Li et al.<sup>[14]</sup> found that the oxidation stability of 0.7 mol L<sup>-1</sup> lithium bisoxalate borate (LiBOB)-sulfolane (TMS)/dimethyl carbonate (DMC) electrolyte was 5.3 V, and when it was applied to  $\text{Li}||\text{LiNi}_{0.5}\text{Mn}_{1.5}\text{O}_4$  battery, it showed great cycle stability, low impedance and excellent rate performance, but its low-temperature performance needed to be improved. Xue et al.<sup>[15]</sup> reported that a single sulfone electrolyte can be greatly compatible with graphite but not with high-voltage cathode materials. When EMS and DMC were mixed, it made  $\text{Li}||\text{LiNi}_{0.5}\text{Mn}_{1.5}\text{O}_4$  batteries maintain 97% capacity retention after 100 cycles, and its columbic efficiency was higher than 99%. On the other hand, in terms of lithium salt, although lithium hexafluorophosphate ( $\text{LiPF}_6$ ) has been widely used in current commercial electrolytes, it is extremely easy to absorb water to deteriorate, and has poor low-temperature performance and thermal instability. Therefore, new organic lithium salts such as  $\text{LiTFSI}$ ,<sup>[16]</sup>  $\text{LiFSI}$ ,<sup>[17]</sup> and  $\text{LiDFOB}$ <sup>[18]</sup> have begun to receive extensive attention. However, sulfonamide lithium salts have the advantages of outstanding thermal stability and high ionic conductivity, while their strong corrosive effect on the cathode collector aluminum (Al) foil at about 4 V also limits their application in the high-voltage field to a certain extent. In recent years, HCE<sup>[17b,19]</sup> has become a hot research topic. It is believed that due to the special properties of HCE,

S. S. Lin, H. M. Hua, P. B. Lai, J. B. Zhao  
State-Province Joint Engineering Laboratory of Power Source Technology for New Energy Vehicle  
Engineering Research Center of Electrochemical Technology  
Ministry of Education  
College of Chemistry and Chemical Engineering  
Xiamen University  
Xiamen 361005, P. R. China  
E-mail: jbzha@xmu.edu.cn

 The ORCID identification number(s) for the author(s) of this article can be found under <https://doi.org/10.1002/aenm.202101775>.

DOI: 10.1002/aenm.202101775

the cathode/electrolyte interface (CEI) layer containing a large amount of lithium fluoride (LiF) can effectively inhibit the corrosion of Al collector,<sup>[20]</sup> which greatly broadens the application range of this type of lithium salt. On the other hand, HCE still has certain shortcomings, such as high viscosity, low ion conductivity, and high lithium salt cost, which also limits its industrial application. The LHCE<sup>[21]</sup> is an improvement based on the HCE, that is, adding a “diluent”<sup>[22]</sup> that does not coordinate with Li<sup>+</sup> in the solution to reduce the apparent concentration. This not only ensures that the bulk microstructure of the electrolyte is not destroyed, but also reduces the viscosity and economic cost of the electrolyte and improves the ion conductivity, which increases more possibilities for its commercialization.

In our work, we firstly selected the cheap and commonly used sulfone solvent TMS<sup>[24]</sup> and carboxylate solvent EA<sup>[11c]</sup> with high ionic conductivity, low viscosity, and low freezing point, and mixed them at a volume ratio of 3:7. LiTFSI and LiDFOB with high ionic conductivity and good low-temperature performance were selected as lithium salts. Two kinds of TMS/EA-based HCEs including TE-5m-LiTFSI and TE-4m-LiTD (4.3:1 by mole) were designed by combining theoretical calculation with experiments. They can both make Li||NCM523 batteries maintain ≈83% capacity retention when charged to 4.6 V under 1 C (1 C = 200 mA g<sup>-1</sup>) current density at 25 °C, showing good high-voltage cyclic stability. Considering the high viscosity, low ionic conductivity, and high economic cost of HCE, we tried to add HFE inert solvent to further optimize the electrolyte. However, we observed that HFE can maintain a similar microscopic state like the HCEs, but there are significant differences in electrochemical properties. That is, single-salt LHCEs were completely unable to achieve electrochemical performance similar to the pristine HCEs, but the dual-salt LHCEs can maintain to a certain degree. Based on theoretical simulation and experimental results, we found that the dominant contact ion pairs (CIPs) and ion aggregate ion pairs (AGGs) in the diluted HCEs were separated by HFE, that is, the 3D network structure in the HCEs was separated into island-like solvation complex<sup>[23]</sup> in the LHCEs, and the HOMO level of the anions decreased, which made the proportion of inorganic components in the passivation film decreased, so that the high voltage stability cannot be maintained. However, LiDFOB, a good cathode additive, exists in the dual-salt LHCEs. Due to its preferential film formation, the original electrochemical performance was maintained to a certain degree. Furthermore, a modified dual-salt LHCE, TEH-2m-LiTD with 10 wt% fluorocarbonate (FEC), was obtained. It made Li||NCM523 batteries maintain ≈89% capacity retention under the same conditions as before; And the rate performance is also very superior, even under the condition of 10 C current density can still discharge ≈65% mass-specific capacity (130 mAh g<sup>-1</sup>). What's more, Li||Cu half-cells with the electrolyte can stabilize for 200 cycles and keep ≈97.5% coulombic efficiency with the current density of 1 and 1 mAh cm<sup>-2</sup> lithium depositing amount, showing good compatibility with lithium metal anode. Not only that, the electrolyte can still remain liquid state and has decent ionic conductivity even at -80 °C, thus making Li||NCM523 battery deliver ≈75% room capacity under the condition of 4.6 V and 0.1 C at -40 °C, and fast charge/discharge for 200 cycles with 1 C current density, showing excellent low-temperature performance.

In conclusion, this work provides a new idea for the design of fast-dynamic, high-voltage, and low-temperature electrolyte.

## 2. Results and Discussion

First, we prepared a series of LiTFSI single-salt TMS/EA-based electrolytes with different concentrations, and characterized their ionic conductivity and viscosity at room temperature of 25 °C (Figure 1a). It was found that ionic conductivity and viscosity of these electrolytes were basically negatively correlated, and they changed sharply after 4m. In addition, it is important to note that the ionic conductivity of TE-1 m-LiTFSI electrolyte was similar with commercial 301 electrolyte (EC/DMC-1M-LiPF<sub>6</sub>), while its viscosity and contact angle with separator is superior to the latter (Figure S1, Supporting Information), showing that the addition of EA does benefit to reduce the electrolyte viscosity and improve ionic conductivity. (Table S1, Supporting Information) After adding a certain amount of HFE inert solvent to dilute the electrolyte, the electrolyte viscosity decreased sharply and the ionic conductivity almost had no change, which is also the result we expected. Through the characterization of <sup>7</sup>Li-NMR, it can also be observed that within a certain concentration range, the chemical shift gradually moves to higher field as the concentration increases, indicating the enhancement of solvation around Li<sup>+</sup>. (About 0.2 ppm chemical shift is Li<sup>+</sup> from 0.1 m LiClO<sub>4</sub> dissolved in the D<sub>2</sub>O solution, which is used for locking field.) Fourier Transform Infrared Spectroscopy (FT-IR) characterization results also show that the wavelength of the corresponding characteristic groups moves to a higher wave number, that is “blue shift”, indicating that the interaction between both solvent and anion and Li<sup>+</sup> is boosted, which is also verified with the results characterized by <sup>7</sup>Li-NMR. MD results (Figure 1d–f, Supporting Information computational details) show that as the electrolyte concentration increases, the number of Li<sup>+</sup> coordinated with solvent molecules reduces from 4–5 to 2–3, and when it is more than 5 m, TFSI<sup>-</sup> anionic coordination number gradually increases to ≈2 and keep stable, suggesting TFSI<sup>-</sup> enter the inner of solvation layer. In LHCEs, the coordination number of HFE is nearly zero, indicating the addition of HFE did not coordinate with Li<sup>+</sup> and change the coordination situation of pristine HCEs. We can also see that the micro-state of LHCE is more similar to that of HCE, and very different from that of the dilute one, which is what we hope. (Figure 1g, Supporting Information computational details) And it is worth noting that, of course, the HFE diluent does not greatly change the bulk phase structure of LHCEs, but the state of the electrolyte at the interface may be different, and therefore the consistency of its electrochemical properties before and after is not guaranteed. (Electrochemical properties will be discussed in more detail later)

On the other hand, we have partly substituted LiDFOB for LiTFSI in the hope of achieving similar or better electrochemical properties. Based on the previous experimental results, we fixed the total molarity of LiTFSI and LiDFOB as 4 m, prepared the electrolytes according to different mole ratios and characterized the changes in ionic conductivity and viscosity (Figure 2a). As the results have shown, with the gradual increase of the proportion of LiDFOB, the ionic conductivity

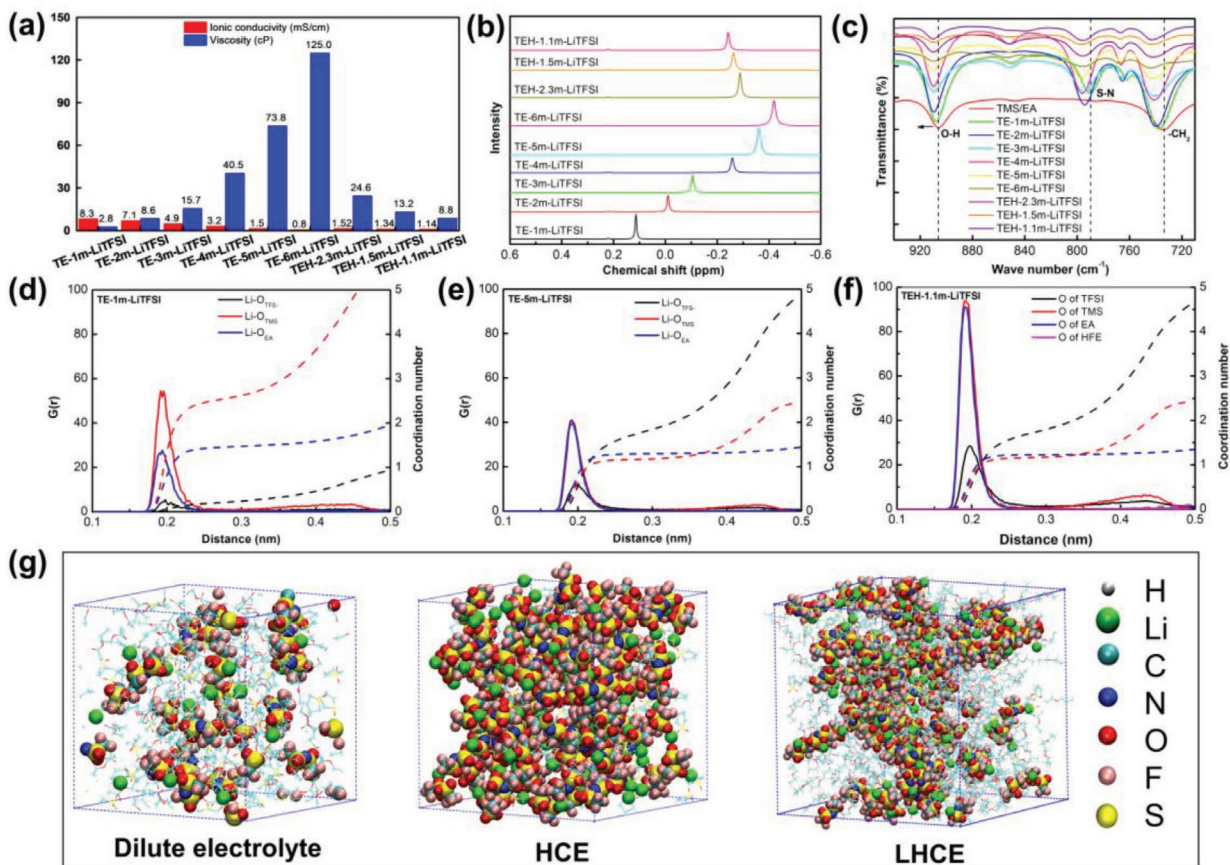


**Figure 1.** a) Ionic conductivity and viscosity of nine electrolytes at room temperature of 25 °C. b)  $^7\text{Li}$ -NMR comparison results of nine electrolytes at room temperature of 25 °C. c) FT-IR spectrum of several electrolytes at 25 °C. d–f) Radial distribution function of dilute electrolyte (TE-1m-LiTFSI), HCE (TE-5m-LiTFSI), and LHCE (TEH-1.1m-LiTFSI). g) Molecular dynamics (MD) simulation results of dilute electrolyte (TE-1m-LiTFSI), HCE (TE-5m-LiTFSI), and LHCE (TEH-1.1m-LiTFSI).

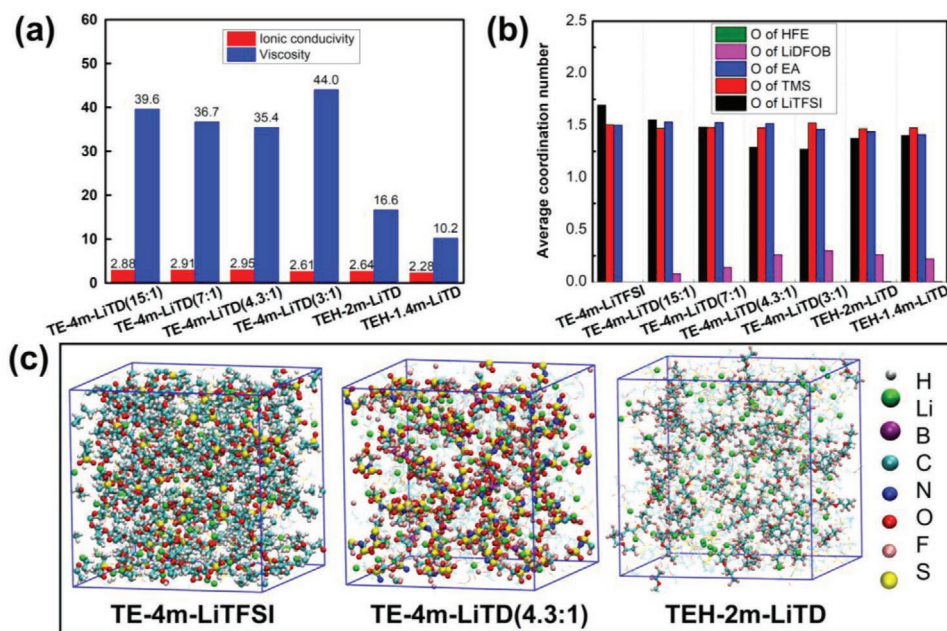


**Figure 2.** a) Ionic conductivity and viscosity of different dual-salt HCEs and LHCEs at 25 °C. b) Average coordination number of each component of the solvation structure of single-salt and dual-salt HCEs and LHCEs. c) MDs simulation results of three electrolytes, TE-4m-LiTFSI, TE-4m-LiTD (4.3:1), and TEH-2m-LiTD.

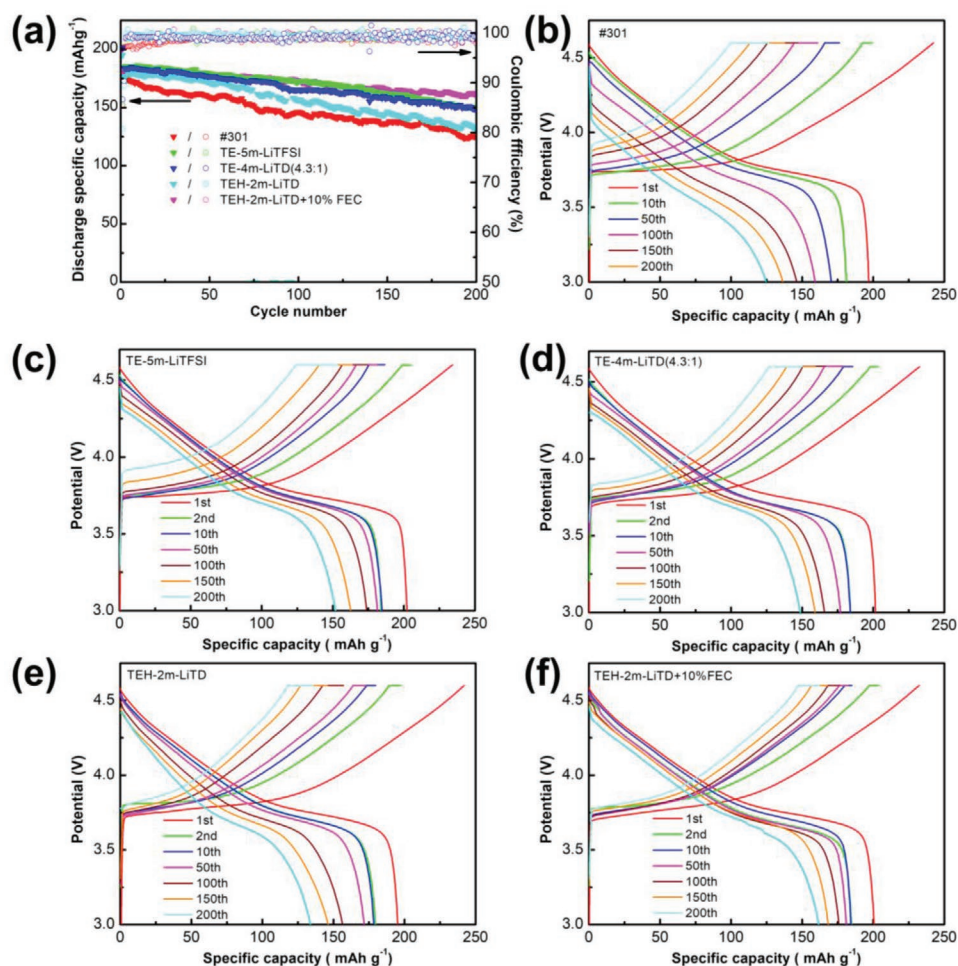


**Figure 3.** Electrochemical performance of Li||NCM523 batteries with five kinds of electrolytes. a) Cyclic performance of Li||NCM523 batteries with five kinds of electrolytes at a cut-off voltage of 4.6 V and current density of 1 C ( $1\text{ C} = 200\text{ mA g}^{-1}$ ). b–f) Voltage-mass specific capacity curves for the cycles specified in (b) commercial 301 electrolyte, c) TE-5m-LiTFSI, d) TE-4m-LiTD (4.3:1), e) TEH-2m-LiTD, and f) TEH-2m-LiTD +10%FEC, respectively.

of electrolytes slightly increased first and then decreased, while the change trend of the viscosity was just the opposite. We think that the addition of LiDFOB may change the microstructure of electrolytes, and then cause the difference of the physical properties of electrolytes. We also carried out the theoretical calculation and MD simulation analysis of the electrolytes (Figure 2b,c, and Supporting Information computational details). It can be seen that when the concentration of LiDFOB was low (less than 0.5 m), the binding of LiTFSI with  $\text{Li}^+$  was still very tight. However, when the molarity further increased ( $\geq 0.75\text{ m}$ ), it is obvious that LiTFSI was partly replaced, thus affecting its physical and chemical properties, which is also consistent with the corresponding characterization and test results. As a result, TE-4m-LiTD (4.3:1) was selected for subsequent performance studies with a certain amount of HFE dilution. Limited by the solubility of lithium salt, we obtained two kinds of dual-salt LHCEs including TEH-2m-LiTD and TEH-1.4m-LiTD. Similarly, the physical property characterization (Figure 2a) revealed that the viscosity of the diluted electrolyte decreased significantly and the ionic conductivity also decreased to a certain extent.

To test the electrochemical performance of above electrolytes, we applied them to Li||NCM523 batteries charged to 4.6 V at a current density of 1 C (Figure 3 and Figures S4–S6, Supporting Information). The results show that: Compared with the traditional commercial 301 electrolyte (Figure 3b), single-salt HCE, TE-5m-LiTFSI, (Figure 3c) shows obvious superiority in performance. However, when the concentration is too high (Figure S4c, Supporting Information), it will also be detrimental to the performance; and when the concentration is too low (Figure S4b, Supporting Information), its anti-oxidation is relatively poor, overcharging occurs after a certain number of cycles, so a moderate concentration is also very important. However, when the proportion of LiDFOB rises to a certain level, even if the concentration is low (4 m), it can still maintain good electrochemical performance. (Figure 3d and Figure S5, Supporting Information) Namely, TE-4m-LiTD (4.3:1), a dual-salt HCE, can also make Li||NCM523 batteries own  $\approx 83\%$  capacity retention at the same condition similar with the single-salt one. We believe that this is mainly due to the good film-forming properties of LiDFOB, which contributes to the improvement of electrolyte oxidation stability. On the other

hand, from the electrochemical performance of two types of LHCEs (Figure 3e and Figure S6, Supporting Information), we have obtained completely different experimental results: all of the single-salt LHCEs from TE-5m-LiTFSI make Li||NCM523 batteries overcharged at around 4.5 V, which is also consisted with the linear scan voltammetry (LSV) characterization on the Super P-PVDF/Al working electrode. (Figure S3, Supporting Information) We believe that the addition of HFE aggravates the corrosion of Al current collector by LiTFSI. While another type of dual-salt LHCE still maintained the electrochemical performance to a certain extent, and had a little performance degradation compared to the original HCE (TE-4m-LiTd). We think the possible reason for the above difference can be that the HFE dilution makes the electrolyte still retain the bulk structure characteristics like HCEs, because HFE hardly interacts with the solvent or lithium salt; while it can break the network of solution, and CIPs and aggregation ion pairs (AGGs) are divided. If so, it is very likely to cause the uneven formation of the passivation film on the cathode surface and reduce the corrosion resistance of Al foil by LiTFSI, therefore the electrolytes

cannot maintain stability at all. On the other hand, with the addition of LiDFOB, a good cathode film-forming additive, the dual-salt electrolytes can preferentially produce a passivation film containing B-containing components to inhibit Al corrosion and realize relatively good high-voltage cyclic stability to some extent. Furthermore, a certain amount of FEC was added to optimize. On the one hand, it has lower HOMO value to improve the high-voltage stability of the whole electrolyte. On the other hand, its synergistic effect with LiDFOB can modify the uniformity of CEI film so as to optimize the electrochemical stability of batteries. As the results have shown that the addition of 10 wt% FEC enables Li||NCM523 batteries to maintain a capacity retention of nearly 89% after 200 cycles, which is in line with our expected results. (Figure 3f and Figure S7, Supporting Information)

To further understand the mechanism of electrolytes on the NCM523 cathode surface, we carried out the characterization tests of TEM and XPS. (Figure 4) First of all, by comparing with TEM morphology of NCM523 cathode cycled for 20 times in different electrolytes, we can find that the CEI layer

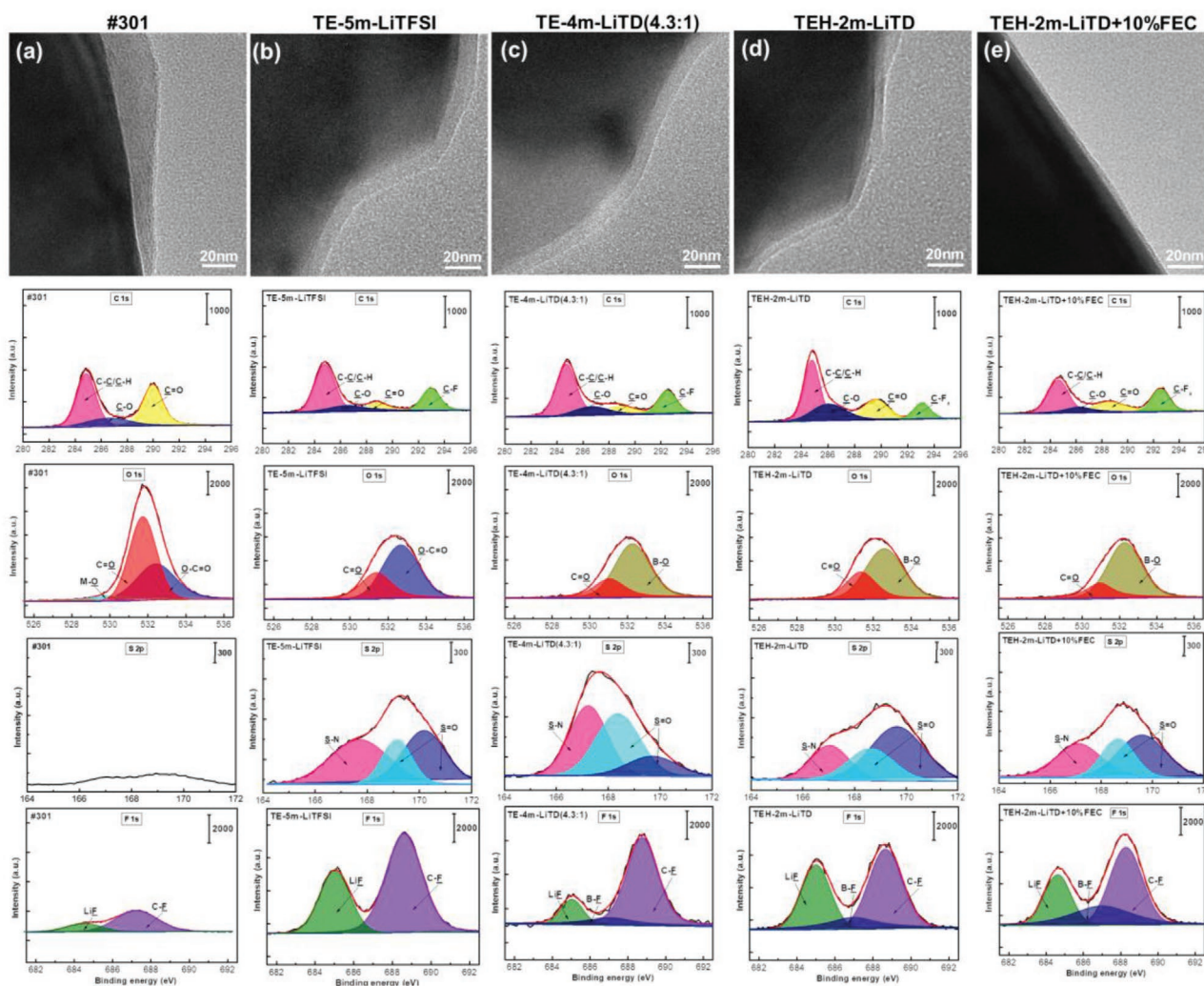


**Figure 4.** TEM images and XPS characterization test results of Li||NCM523 full-batteries with five different electrolytes after 20 cycles. a) commercial 301 electrolyte. b) TE-5m-LiTFSI. c) TE-4m-LiTd (4.3:1). d) TEH-2m-LiTd. e) TEH-2m-LiTd+10%FEC.

generated from commercial 301 is quite uneven; and as C 1s, O 1s, S 2p, and F 1s spectrum of XPS analysis shown, its composition mainly includes alkoxy lithium (LiOR, 530.9 eV, O 1s) and lithium carbonate ( $\text{Li}_2\text{CO}_3$ , 288.5 eV, C 1s and O 1s, 532 eV) and a small amount of lithium fluoride (LiF, 684.9 eV, F 1s), suggesting organic components generated by solvent decomposition are dominant, which is not conducive to protecting the cathode materials at 4.6 V. What's more, M-O (O 1s, 530 eV) signal was also detected on the cathode surface, indicating there may be dissolution of transition metal during the cycling, which is also harmful to cyclic stability. As for TE-5m-LiTFSI, it generated a relatively uniform CEI layer of  $\approx 9$  nm mainly composed of inorganic components like LiF and lithium sulfonate, suggesting TFSI<sup>-</sup> anion was indeed involved in formation of CEI film. As for the dual-salt HCE, TE-4m-LiTD (4.3:1), the introduction of LiDFOB led to more B-containing species (B-O and B-F) in CEI composition, and reduced the proportion of organic components, which is also beneficial to protect cathode materials. After adding HFE into TE-4m-LiTD, the CEI film became a little uneven and the proportion of LiF significantly increased and so did organic components, we think this might be due to the decomposition of HFE. Of course, HFE decomposing is not helpful to the high-voltage stability, thus degrading its electrochemical performance compared with the dual-salt HCE. And it is because of the absence of LiDFOB that single-salt HCE (TE-5m-LiTFSI) was completely unable to maintain electrochemical performance after dilution by adding HFE, more intuitively explaining the importance and indispensability of LiDFOB in the LHCEs. However, when adding 10 wt% FEC to further optimize dual-salt TEH-2m-LiTD, the CEI layer was only about  $\approx 5$  nm thick and very uniform, and the proportion of organic components greatly decreased. We believe that FEC has lower HOMO value to enhance the antioxidation of whole electrolyte, and it can also synergy with LiDFOB to optimize the composition of passivation film, offering more assurance to improve cyclic stability of batteries. On the other hand, FEC is also an outstanding anode film-forming additive to protect lithium metal anode.<sup>[24]</sup> We applied the electrolyte to Li||Cu half-cells, and the coulombic efficiency can reach  $\approx 97.5\%$  after 200 cycles under the current density of  $1 \text{ mA cm}^{-2}$  and lithium deposition amount of  $1 \text{ mAh cm}^{-2}$ , proving its superiority of compatibility with lithium anode. (Figure 7d)

In order to confirm the effect of different electrolytes on the NCM523 cathode materials under 4.6 V, we compared the cross-sectional SEM images of cathode materials before and after 200 cycles. As we can see, there was basically no crack inside the pristine NCM523 materials which were composed of spherical secondary particles with an average diameter of  $\approx 5 \mu\text{m}$  compiled by primary particles. After 200 cycles, with commercial 301 electrolyte (Figure 5a), the interior material appeared obvious breakage, which indicated the electrolyte could not protect the material sufficiently under the high voltage of 4.6 V. And TEH-2m-LiTD (Figure 5d) had an adverse effect only second to the former, which was consistent with the cyclic performance. While TE-5m-LiTFSI (Figure 5b) and TE-4m-LiTD (4.3:1) (Figure 5c) just caused some slighter cracks inside NCM523 cathode materials, and TEH-2m-LiTD+10%FEC (Figure 5f) did the least damage, suggesting the electrolyte plays a good role in inhibiting deterioration of materials during charging and

discharging process. As the XRD results of NCM523 material before and after for 200 cycles shown (Figure 5g), (003) peak of NCM523 cathode moved to lower angle with traditional commercial 301 electrolyte. As we all know, this peak shift is an indicator of irreversible phase transition of NCM523 cathode material, corresponding to the battery electrochemical performance. However, it can be seen that other four electrolytes move more or less, but the degree of irreversibility is not so serious, which further proves that the modified electrolyte has an obvious protective effect on cathode materials. In addition, the interfacial impedance value of Li||NCM523 batteries with traditional commercial 301 electrolyte is still relatively high, suggesting its properties are not very stable. In conclusion, all of the characterization results are in good agreement with the electrochemical properties. (Figure 5h–j)

What's more, rate performance of Li||NCM523 batteries with TEH-2m-LiTD+10%FEC was studied. (Figure 6a) To our surprise, Li||NCM523 batteries can remain  $\approx 65\%$  of mass-specific capacity even at an ultra-high current density of 10 C, and when returned to 0.1 C, it can recover as before ( $\approx 200 \text{ mAh g}^{-1}$ ), behaving a very superior fast-dynamic performance. While the batteries using commercial 301 electrolyte just delivered 60% of capacity ( $\approx 120 \text{ mAh g}^{-1}$ ) only at 2 C, and when current density was increased to 10 C, merely  $\approx 15\%$  ( $\approx 30 \text{ mAh g}^{-1}$ ) remained, having no advantage of fast-charging/discharging at all. We believe the two electrolytes cause such a large difference in rate performance mainly due to the following points: 1) Although the conductivity of TEH-2m-LiTD+10%FEC is less than  $3 \text{ mS cm}^{-1}$  at room temperature, and commercial 301 electrolyte reaches  $10.8 \text{ mS cm}^{-1}$ ; while the contact angle of commercial electrolyte with Celgard separator is  $50.4^\circ$ , and ours is  $36.3^\circ$ , which is obvious that our electrolyte has a better wettability with separator than the former. The Electrochemical impedance spectroscopy (EIS) result of 2016-type batteries made up of the electrolyte and separator were used to characterize the electrolyte conductivity closer to the real system, and their gap has narrowed to about 1.5 times (Figure 6b). 2)  $\text{Li}^+$  transference number of commercial 301 electrolyte is only 0.27, while our electrolyte is close to 0.7 (0.68), which is much beneficial to  $\text{Li}^+$  diffusion in the bulk electrolyte. 3) Temperature-dependent EIS curves of Li||NCM523 batteries with commercial 301 electrolyte and TEH-2m-LiTD+10%FEC were respectively tested to calculate the activation energy. (Figure 6d) ( $E_{a,\text{SEI}}$  relates to two processes of  $\text{Li}^+$  desolvation at the electrolyte/electrode interfaces and  $\text{Li}^+$  transporting through SEI, and  $E_{a,\text{ct}}$  means the activation of  $\text{Li}^+$  diffusion within NCM523 cathode.) (Figure 6e,f) As the results shown, the activation energy of Li||NCM523 with commercial 301 electrolyte required in any process is higher than that of TEH-2m-LiTD+10%FEC. All in all, there is no doubt that our optimized LHCE has more advantages than commercial 301 electrolyte in fast-dynamics.

On the other hand, attributed to the low freezing point of EA, to our surprise, even with TMS which is a high-freezing point solvent to keep solid at room temperature, the TMS/EA-based electrolytes we designed also show very excellent performance even at  $-60^\circ\text{C}$ . (Figure S7, Supporting Information) While the commercial 301 electrolyte has obvious solidification and a sharp drop in ion conductivity at only about  $-30^\circ\text{C}$ . (Figure 7a) It needs to be emphasized that our final optimized

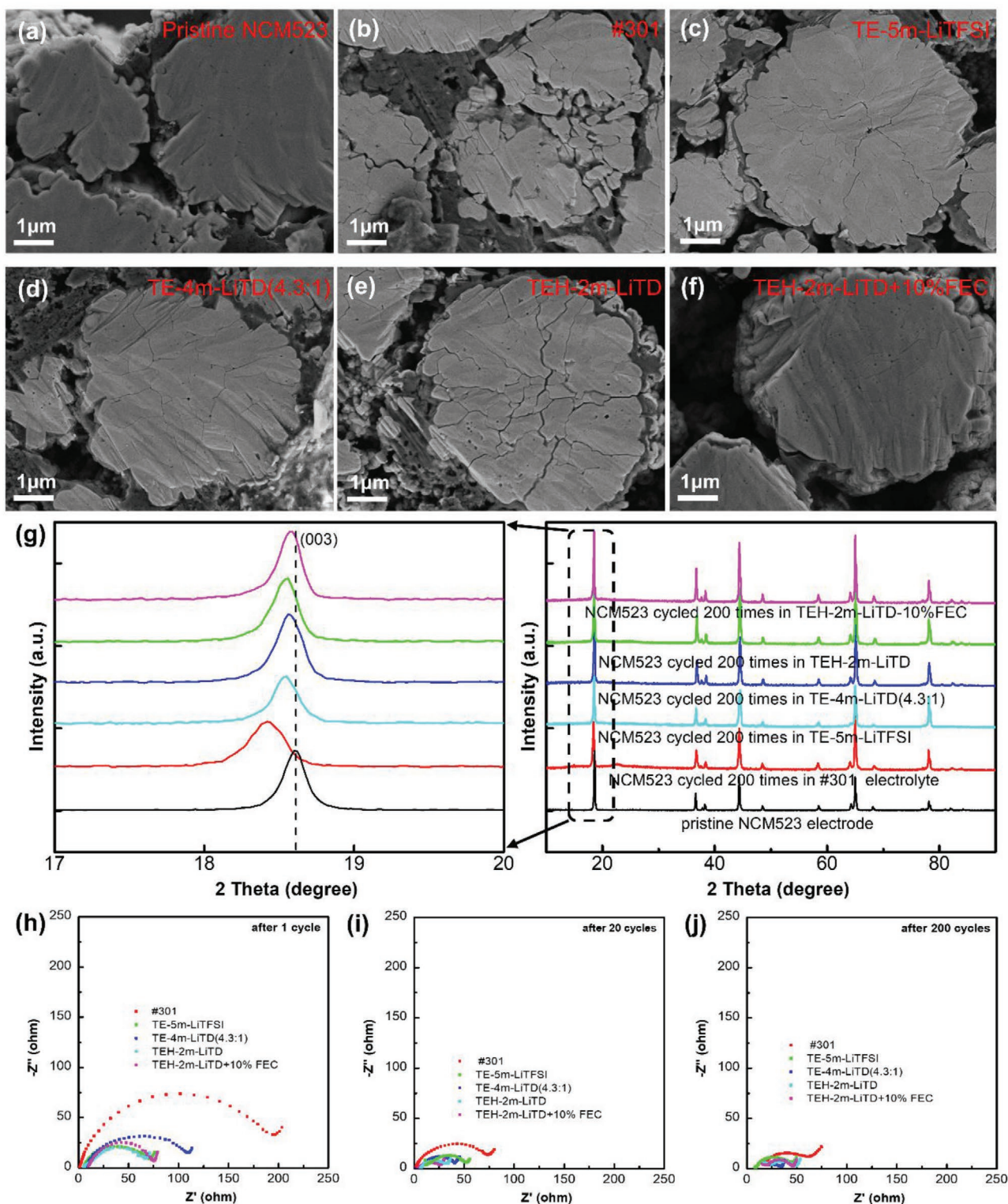


**Figure 5.** a–f) NCM523 cathode material cross-sectional SEM images of Li||NCM523 full-batteries with five different electrolytes before and after 200 cycles. g) XRD characterization results of NCM523 cathode material in Li||NCM523 batteries with five electrolytes cycled before and after 200 times. h–j), Interface impedance curves of Li||NCM523 batteries with five electrolytes for h) 1 cycle. i) 20 cycles and j) 200 cycles.

design of TEH-2m-LiTD+10%FEC can remain liquid state even at  $-80\text{ }^{\circ}\text{C}$  and has a decent ionic conductivity. We tested the charging/discharging curves of Li||NCM523 containing

TEH-2m-LiTD+10%FEC electrolyte with several current densities charged to 4.6 V at  $-40\text{ }^{\circ}\text{C}$ , and we can see it still exceeds 75% ( $102\text{ mAh g}^{-1}$ ) of room temperature discharge specific

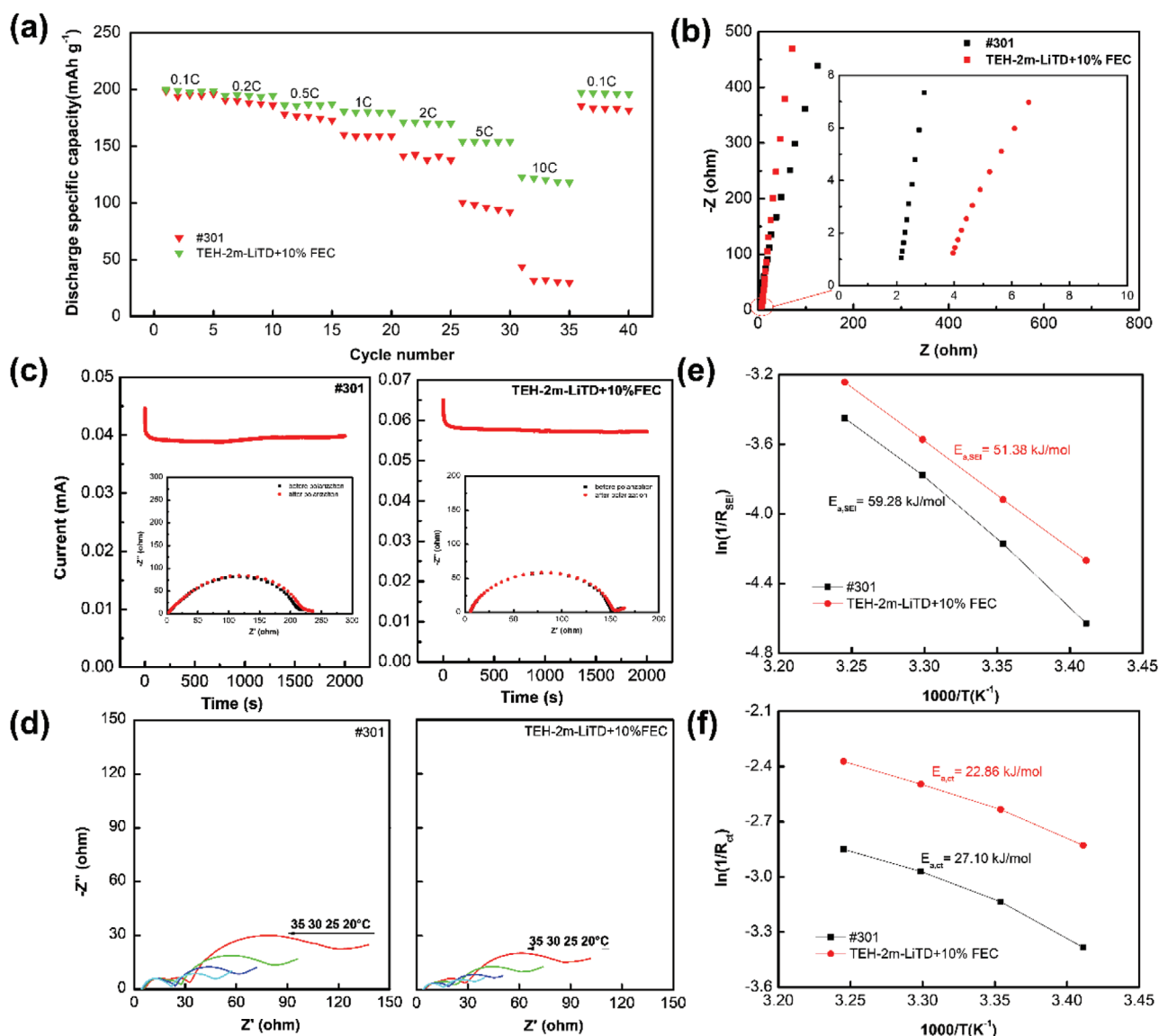


**Figure 6.** a) Rate performance of Li||NCM523 batteries with commercial 301 electrolyte and TEH-2m-LiTD+10%FEC with a cut-off voltage of 4.6 V at 25 °C. b) EIS curves of batteries containing separator and stainless steel with commercial 301 electrolyte and TEH-2m-LiTD+10%FEC, respectively. c) Chronoamperometry for Li<sup>+</sup> transference number ( $t_{Li^+}$ ) of commercial 301 electrolyte and TEH-2m-LiTD+10%FEC, respectively; d) Temperature-dependent EIS curves of Li||NCM523 batteries with commercial 301 electrolyte and TEH-2m-LiTD+10%FEC. e, f).  $\ln(R^{-1})-T^{-1}$  curve is obtained by fitting the  $R_{SEI}$  and  $R_{CT}$  of the battery with commercial 301 electrolyte and TEH-2m-LiTD+10%FEC, respectively.

capacity at 0.1 C. Even more surprising is that it can stabilize for 200 cycles with 1 C under a cut-off voltage of 4.6 V at -40 °C, showing very excellent low-temperature fast dynamics. By the way, the electrolyte not only does benefit NCM523 cathode materials, but also has very good cyclic reversibility for lithium metal (Figure 7d) and graphite (Figure S9, Supporting Information) anode materials, exhibiting dual compatibility with both positive and negative electrodes.

### 3. Conclusion

In our work, two kinds of TMS/EA-based HCEs, TE-5m-LiTFSI, and TE-4m-LiTD (4.3:1), were designed by combining

theoretical calculation and experiments at first, and finally an optimized LHCE, TEH-2m-LiTD +10%FEC, was obtained by adding a certain amount of HFE dilution and 10 wt% FEC additive. This electrolyte makes Li||NCM523 batteries maintain a capacity retention of  $\approx 89\%$  for 200 cycles under a cut-off voltage of 4.6 V with 1 C (200 mA g<sup>-1</sup>) current density at room temperature, and rate performance is also outstanding to deliver  $\approx 65\%$  ( $\approx 130$  mAh g<sup>-1</sup>) capacity at 10 C. What's more, even at a low temperature of -40 °C, it can still make Li||NCM523 stabilize for 200 cycles with 1 C current density, showing excellent low-temperature fast-charging/discharging performance. On the other hand, it makes Li||Cu half-cells obtain relatively decent depositing/stripping columbic efficiency of  $\approx 97.5\%$  after 200 cycles at the current density of 1 mA cm<sup>-2</sup> and the Li

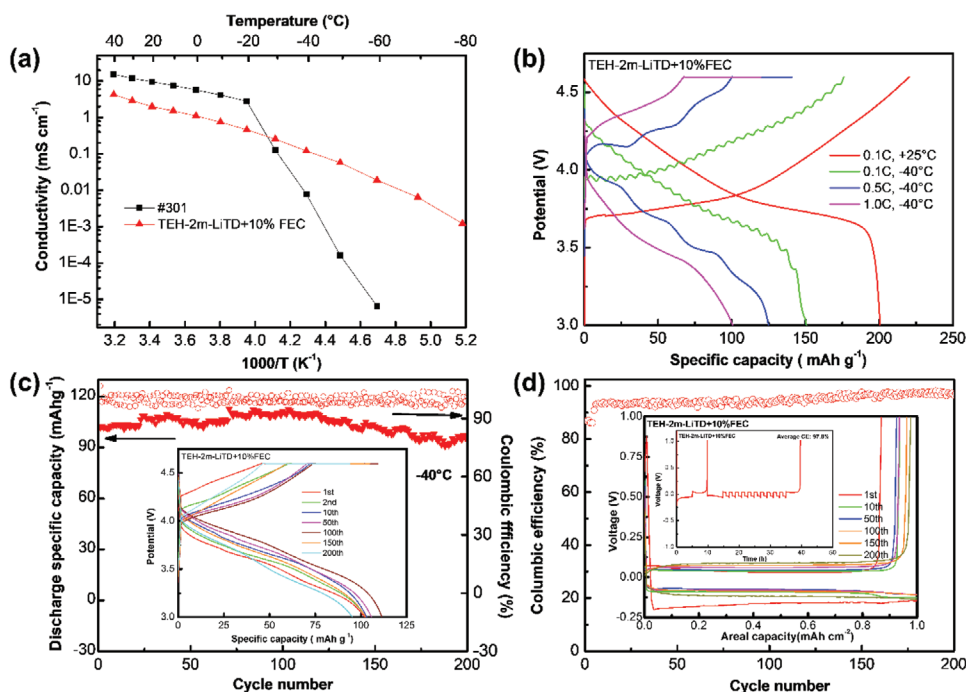


**Figure 7.** a) Ionic conductivity of two electrolytes at different temperatures. b) Voltage-specific capacity curve for first cycle of Li||NCM523 batteries with TEH-2m-LiTD+10%FEC at 25 and  $-40\text{ }^{\circ}\text{C}$ . c) Electrochemical performance of Li||NCM523 batteries with TEH-2m-LiTD+10%FEC charged to 4.6 V at a current density of 1 C ( $1\text{ C} = 200\text{ mA g}^{-1}$ ) at  $-40\text{ }^{\circ}\text{C}$ . d) Cyclic performance of Li||Cu half-batteries with TEH-2m-LiTD+10%FEC at a current density of  $1\text{ mA cm}^{-2}$  and the deposition amount of  $1\text{ mAh cm}^{-2}$ .

depositing amount of  $1\text{ mAh cm}^{-2}$ , and has good compatibility with graphite anode as well. To sum up, this work provides a new idea for the design of high-voltage, fast dynamics, and low-temperature electrolyte. And an LHCE directly from the best HCE is not advisable, diluent and additive should cooperate to optimize.

#### 4. Experimental Section

**Material Preparation:**  $\text{LiNi}_{0.5}\text{Co}_{0.2}\text{Mn}_{0.3}\text{O}_2$  (NCM523) or graphite active electrode material, acetylene black conductive agent, and PVDF binder were weighed according to the mass ratio of 8:1:1 and grinded to make them uniform. *N*-methyl-2-pyrrolidone was used as solvent to adjust consistency, and then the slurry was electromagnetically stirred for 6 h. After that, the slurry was coated on the Al foil or copper (Cu) foil and left them on the heating plate for about 30 min. Finally, put them in a vacuum oven at  $80\text{ }^{\circ}\text{C}$  for 12 h. The loading amount of active cathode material is about  $5\text{ mg cm}^{-2}$ . Super P-PVDF-Al working electrode was made according to the method as before just without active cathode materials (NCM523). The preparation of the electrolytes was to firstly mix TMS and EA at a volume ratio of 3:7, and then dissolve a certain amount of LiTFSI in the mixed solvent to obtain six single-salt HCEs of 1–6 m. Add HFE into TE-5m-LiTFSI according to  $n_{\text{LiTFSI}}:n_{\text{HFE}} = 1:1, 1:2, 1:3$  to obtain TEH-2.3m-LiTFSI, TEH-1.5m-LiTFSI and TEH-1.1m-LiTFSI. Use 0.25 m, 0.5 m, 0.75 m, 1.0 m LiDFOB to replace equal molarity of LiTFSI to obtain TE-4m-LiTD( $x:1$ ) ( $x = 15, 7, 4.3, 3$ ) four kinds of dual-salt HCEs. Add a certain amount of diluent HFE to TE-4m-LiTD (4.3:1) to obtain TEH-2m-LiTD and TEH-1.4m-LiTD. 5, 10, and 15 wt% FEC were added into TEH-2m-LiTD to obtain TEH-2m-LiTD+5%FEC, TEH-2m-LiTD+10%FEC, TEH-2m-LiTD+15%FEC.  $0.1\text{ mol L}^{-1}$  (M)  $\text{LiClO}_4$  was dissolved into  $\text{D}_2\text{O}$  to be used for locking field in the  $^7\text{Li}$ -NMR tests. The diameter of the electrode piece and lithium sheet is 12 mm. Celgard

separator was purchased from the manufacturer. The electrolyte was guaranteed to add 75 microliters in total. All of the batteries used for electrochemical characterization were assembled using 2016-type coin cells. And Li||Li symmetrical batteries used for  $\text{Li}^+$  transference number ( $t_{\text{Li}^+}$ ) measurement were 2032-type coin cells.

**Material Characterization:** Rigaku miniflex 600 X-ray diffractometer with Cu K2 target was used to test X-ray diffraction (XRD) data, and its angle range was from  $10^{\circ}$  to  $90^{\circ}$  and scanning speed was  $2^{\circ}\text{ min}^{-1}$ ; Scanning electron microscope (SEM) images were obtained from Zeiss Gemini SEM 500 field emission SEM; Cross section of NCM523 cathode materials was realized by Ion Beam Slope Cutter (Lecia EM TIC 3X). Transmission electron microscopy (TEM) pictures were picked from JEM2100 instrument, X-ray photoelectron spectroscopy (XPS) spectral information was from PHI Quantum 2000 test equipment;  $^7\text{Li}$ -NMR data was taken with Ascend 500 MHz spectrometer at  $25\text{ }^{\circ}\text{C}$ ; FT-IR data was obtained on the infrared spectrometer (ThermoFisher, IS5). Ionic conductivity data of all electrolytes was gotten by conductivity meter (DSC-307A); Viscosity data was measured by the viscometer (VM-10A-L) at  $25\text{ }^{\circ}\text{C}$ ; The contact angle data was tested on the contact angle tester (JC-2000C1) at  $25\text{ }^{\circ}\text{C}$ .

**Electrochemical Characterization:** EIS data was obtained from Solartron Metrology at a frequency range from 0.1 to  $10^5$  Hz. LSV data and cyclic voltammetry were tested with a three-electrode system containing a working electrode of  $1.2 \times 1.2\text{ cm}$  Super P-PVDF/Al working electrode, reference electrode, and counter electrode of Li sheet at a sweeping speed of  $1\text{ mV s}^{-1}$  on the electrochemical workstation (CHI660D). All of the batteries used for electrochemical characterization were assembled in Braun glove box full of Ar gas with water and oxygen content less than 0.1 ppm and then keep still for 12 h. Active material electrodes or Cu foil, a piece of Celgard separator, and Li sheet of 1 mm thick were added to the 2016-type coin cells along with  $75\text{ }\mu\text{L}$  electrolyte in total. And the galvanostatic test data was obtained on the Land BT2000 test system at  $25\text{ }^{\circ}\text{C}$  and on the Neware test system at  $-40\text{ }^{\circ}\text{C}$ , respectively.

## Supporting Information

Supporting Information is available from the Wiley Online Library or from the author.

## Acknowledgements

The authors gratefully acknowledge the financial support of National Key Research and Development Program of China (2017YFB0102000), National Natural Science Foundation of China (21875198, 22021001), the Fundamental Research Funds for the Central Universities (20720190040), Natural Science Foundation of Fujian Province of China (2020J05009) and the key Project of Science and Technology of Xiamen (3502Z20201013). And the authors also would like to express gratitude to the High-throughput Computational Platform of Chinese Materials Genome Engineering for the high-performance computing resources.

## Conflict of Interest

The authors declare no conflict of interest.

## Data Availability Statement

Research data are not shared.

## Keywords

ethyl acetate, fast charging/discharging, high-voltage, LHCE, low temperature, sulfolane

Received: June 9, 2021

Revised: July 13, 2021

Published online:

- [1] M. Winter, B. Barnett, K. Xu, *Chem. Rev.* **2018**, *118*, 11433.
- [2] M. Armand, J. M. Tarascon, *Nature* **2008**, *451*, 652.
- [3] K. Xu, *Chem. Rev.* **2014**, *114*, 11503.
- [4] a) Z. Zhu, D. Yu, Z. Shi, R. Gao, X. Xiao, I. Waluyo, M. Ge, Y. Dong, W. Xue, G. Xu, W.-K. Lee, A. Hunt, J. Li, *Energy Environ. Sci.* **2020**, *13*, 1865; b) X. Ren, X. Zhang, Z. Shadike, L. Zou, H. Jia, X. Cao, M. H. Engelhard, B. E. Matthews, C. Wang, B. W. Arey, X. Q. Yang, J. Liu, J. G. Zhang, W. Xu, *Adv. Mater.* **2020**, *32*, 2004898.
- [5] F. Zhang, S. Lou, S. Li, Z. Yu, Q. Liu, A. Dai, C. Cao, M. F. Toney, M. Ge, X. Xiao, W. K. Lee, Y. Yao, J. Deng, T. Liu, Y. Tang, G. Yin, J. Lu, D. Su, J. Wang, *Nat. Commun.* **2020**, *11*, 3050.
- [6] W. Deng, W. Dai, X. Zhou, Q. Han, W. Fang, N. Dong, B. He, Z. Liu, *ACS Energy Lett.* **2020**, *6*, 115.
- [7] a) Z. Zeng, V. Murugesan, K. S. Han, X. Jiang, Y. Cao, L. Xiao, X. Ai, H. Yang, J.-G. Zhang, M. L. Sushko, J. Liu, *Nat. Energy* **2018**, *3*, 674; b) Y. Sun, Y. Zhao, J. Wang, J. Liang, C. Wang, Q. Sun, X. Lin, K. R. Adair, J. Luo, D. Wang, R. Li, M. Cai, T. K. Sham, X. Sun, *Adv. Mater.* **2018**, *31*, 1806541; c) S. Liu, X. Xia, S. Deng, D. Xie, Z. Yao, L. Zhang, S. Zhang, X. Wang, J. Tu, *Adv. Mater.* **2018**, *31*, 1806470.
- [8] H. Jia, P. Gao, L. Zou, K. S. Han, M. H. Engelhard, Y. He, X. Zhang, W. Zhao, R. Yi, H. Wang, C. Wang, X. Li, J.-G. Zhang, *Chem. Mater.* **2020**, *32*, 8956.
- [9] K. Xu, *Chem. Rev.* **2004**, *104*, 4303.
- [10] Z. Zhang, L. Hu, H. Wu, W. Weng, M. Koh, P. C. Redfern, L. A. Curtiss, K. Amine, *Energy Environ. Sci.* **2013**, *6*, 1806.
- [11] a) Q. Zhao, X. Liu, J. Zheng, Y. Deng, A. Warren, Q. Zhang, L. Archer, *Proc. Natl. Acad. Sci. USA* **2020**, *117*, 26053; b) X. Fan, X. Ji, L. Chen, J. Chen, T. Deng, F. Han, J. Yue, N. Piao, R. Wang, X. Zhou, X. Xiao, L. Chen, C. Wang, *Nat. Energy* **2019**, *4*, 882; c) X. Dong, Z. Guo, Z. Guo, Y. Wang, Y. Xia, *Joule* **2018**, *2*, 902.
- [12] S. Wang, C. Wei, W. Ding, L. Zou, Y. Gong, Y. Liu, L. Zang, X. Xu, *Polymers* **2019**, *11*, 1306.
- [13] S. Tan, Y. J. Ji, Z. R. Zhang, Y. Yang, *ChemPhysChem* **2014**, *15*, 1956.
- [14] A. Abouimrane, I. Belharouak, K. Amine, *Electrochem. Commun.* **2009**, *11*, 1073.
- [15] L. Xue, K. Ueno, S.-Y. Lee, C. A. Angell, *J. Power Sources* **2014**, *262*, 123.
- [16] a) L. Suo, O. Borodin, T. Gao, M. Olguin, J. Ho, X. Fan, C. Luo, C. Wang, K. Xu, *Science* **2015**, *350*, 938; b) K. Xu, C. Wang, *Nat. Energy* **2016**, *1*, 16161; c) C. Yang, J. Chen, X. Ji, T. P. Pollard, X. Lü, C.-J. Sun, S. Hou, Q. Liu, C. Liu, T. Qing, Y. Wang, O. Borodin, Y. Ren, K. Xu, C. Wang, *Nature* **2019**, *569*, 245.
- [17] a) Y. Jie, X. Ren, R. Cao, W. Cai, S. Jiao, *Adv. Funct. Mater.* **2020**, *30*, 1910777; b) J. Qian, W. A. Henderson, W. Xu, P. Bhattacharya, M. Engelhard, O. Borodin, J. G. Zhang, *Nat. Commun.* **2015**, *6*, 6362.
- [18] S. Jiao, X. Ren, R. Cao, M. H. Engelhard, Y. Liu, D. Hu, D. Mei, J. Zheng, W. Zhao, Q. Li, N. Liu, B. D. Adams, C. Ma, J. Liu, J.-G. Zhang, W. Xu, *Nat. Energy* **2018**, *3*, 739.
- [19] a) X. Fan, L. Chen, X. Ji, T. Deng, S. Hou, J. Chen, J. Zheng, F. Wang, J. Jiang, K. Xu, C. Wang, *Chem* **2018**, *4*, 174; b) D. W. McOwen, D. M. Seo, O. Borodin, J. Vatamanu, P. D. Boyle, W. A. Henderson, A. Yamada, *Chem. Commun.* **2013**, *49*, 11194; d) K. Pranay Reddy, P. Fischer, M. Marinaro, M. Wohlfahrt-Mehrens, *ChemElectroChem* **2018**, *5*, 2758.
- [20] K. Matsumoto, K. Inoue, K. Nakahara, R. Yuge, T. Noguchi, K. Utsugi, *J. Power Sources* **2013**, *231*, 234.
- [21] a) Y. Zheng, F. A. Soto, V. Ponce, J. M. Seminario, X. Cao, J.-G. Zhang, P. B. Balbuena, *J. Mater. Chem. A* **2019**, *7*, 25047; b) X. Ren, L. Zou, X. Cao, M. H. Engelhard, W. Liu, S. D. Burton, H. Lee, C. Niu, B. E. Matthews, Z. Zhu, C. Wang, B. W. Arey, J. Xiao, J. Liu, J.-G. Zhang, W. Xu, *Joule* **2019**, *3*, 1662; c) J. Zheng, G. Ji, X. Fan, J. Chen, Q. Li, H. Wang, Y. Yang, K. C. DeMella, S. R. Raghavan, C. Wang, *Adv. Energy Mater.* **2019**, *9*, 1803774; d) X. Ren, S. Chen, H. Lee, D. Mei, M. H. Engelhard, S. D. Burton, W. Zhao, J. Zheng, Q. Li, M. S. Ding, M. Schroeder, J. Alvarado, K. Xu, Y. S. Meng, J. Liu, J.-G. Zhang, W. Xu, *Chem* **2018**, *4*, 1877; e) X. Cao, H. Jia, W. Xu, J. G. Zhang, *J. Electrochem. Soc.* **2021**, *168*, 010522.
- [22] T. Doi, Y. Shimizu, M. Hashinokuchi, M. Inaba, *J. Electrochem. Soc.* **2017**, *164*, A6412.
- [23] S. P. Beltran, X. Cao, J.-G. Zhang, P. B. Balbuena, *Chem. Mater.* **2020**, *32*, 5973.
- [24] X. Li, J. Zheng, X. Ren, M. H. Engelhard, W. Zhao, Q. Li, J.-G. Zhang, W. Xu, *Adv. Energy Mater.* **2018**, *8*, 1703022.